

**Figure S1: Phosphorylation kinetics of phosphorylated CP24**

Immunoblot of isolated thylakoid assayed with anti-P-Thr antibody. Before thylakoid isolation, leaves have been treated with HL ( $1,000 \mu\text{mol photons m}^{-2} \text{ s}^{-1}$ ) for different periods. All lanes were loaded with 3  $\mu\text{g Chl}$ . The immunoblot depicts phosphorylation levels of key proteins including CP43, D2, D1, LhcII, and CP24 at different HL exposure times. **b** Densitometric analysis of immunoblot in (a). Symbols and error bars represent the mean  $\pm$  SD calculated from three independent biological replicates. Western fluorescence intensity is normalized relative to the initial value at time zero.



36

### 37 **Figure S2: Multiple sequence alignment of STN7 from *B. incana* and *A. thaliana***

38 Protein sequences were analyzed with the ESPript 3.0 online software. Chloroplast transport peptides  
 39 determined using ChloroP1.1 online software are marked with black lines below the amino acid sequence.

40

41

42

43

44

45

46

47

48

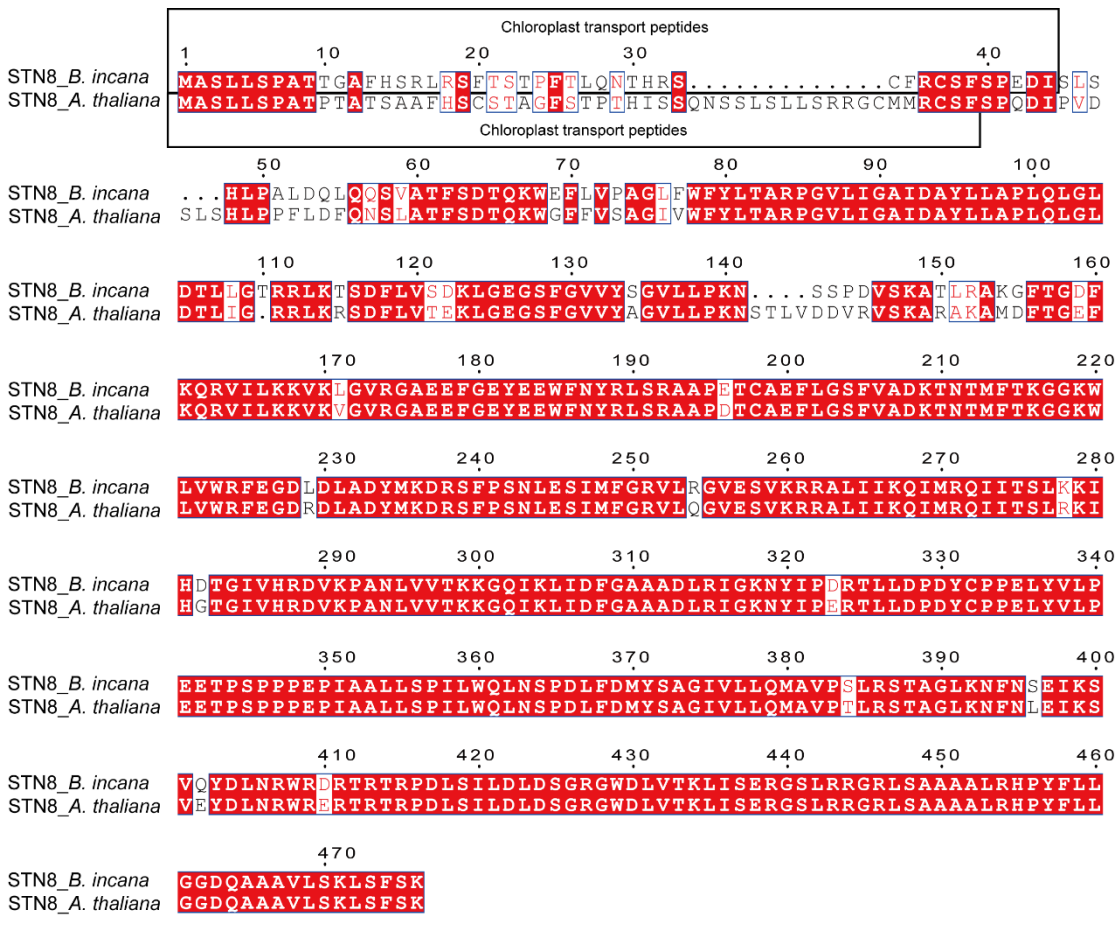
49

50

51

52

53



54

**55 Figure S3: Multiple sequence alignment of STN8 from *B. incana* and *A. thaliana***

56 Protein sequences were analyzed with the ESPript 3.0 online software. Chloroplast transport peptides  
 57 determined using ChloroP1.1 online software are marked with black lines below the amino acid sequence.

58

59

60

61

62

63

64

65

66

67

68

69

70

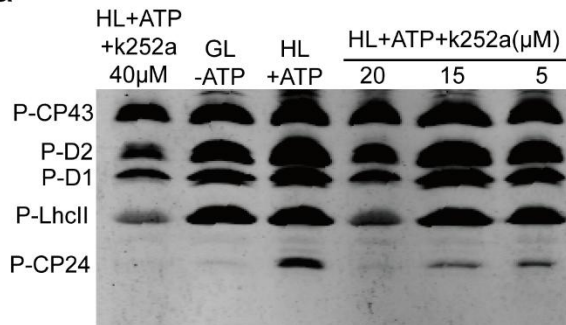
71

72

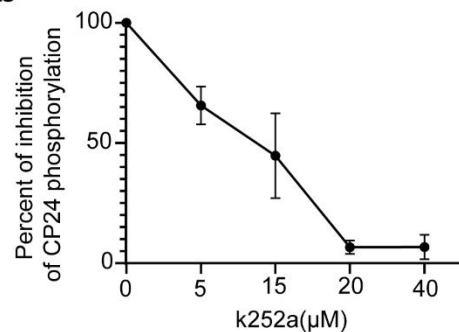
73

74

75

76  
a

b

77 **Figure S4: Inhibition of CP24 phosphorylation with varying concentrations of k252a**78 **a** Immunoblot analysis of chloroplasts exposed to growth light (GL, 100  $\mu\text{mol photons m}^{-2} \text{ s}^{-1}$ ) in the  
79 absence of ATP, and chloroplasts exposed to high light (HL, 1,000  $\mu\text{mol photons m}^{-2} \text{ s}^{-1}$ ) for 30 minutes  
80 in the presence of ATP, or in the presence of ATP and varying concentrations of k252a. The anti-P-Thr  
81 antibody was used to detect phosphorylated proteins. All lanes were loaded with 3  $\mu\text{g Chl}$ . **b** Extent of  
82 CP24 phosphorylation inhibition by k252a. Symbols and error bars represent the mean  $\pm$  SD calculated  
83 from two independent biological replicates.

84

85

86

87

88

89

90

91

92

93

94

95

96

97

98

99

100

101

102

103

104

105

106

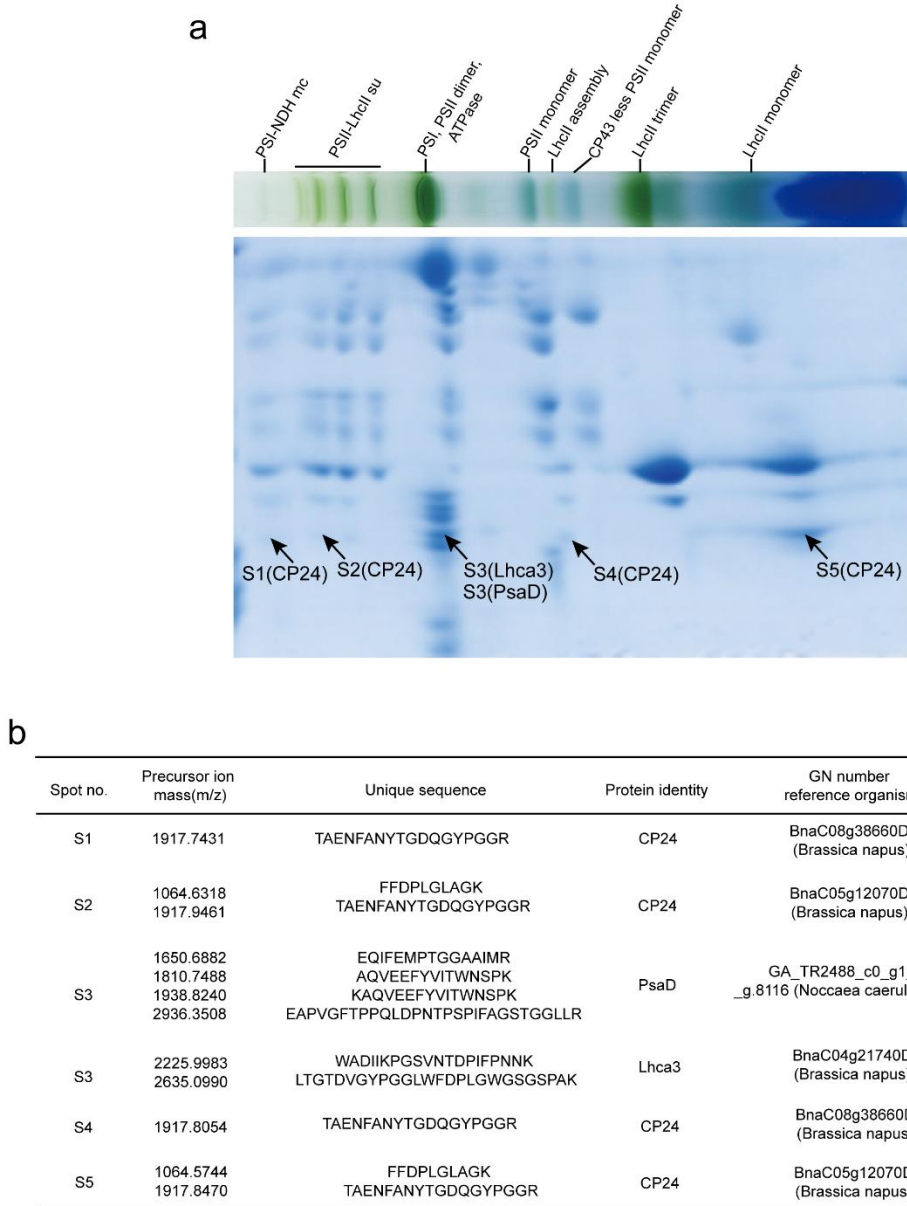
107

108

109

110

111



112

113 **Figure S5: Analysis of proteins corresponding to the position of phosphorylated CP24 in *B. incana***  
 114 **thylakoids by MALDI-TOF-TOF MS/MS following lp-BN/SDS-PAGE**

115 a The thylakoid membrane extracted from GL leaves ( $100 \mu\text{mol photons m}^{-2} \text{ s}^{-1}$ ) were treated with  $\beta$ -  
 116 DM and then complexes were separated by lp-BN/SDS-PAGE. b The proteins corresponding to the  
 117 position of molecular weight of P-CP24 (indicated by the arrow in a) in coomassie blue stain gel were  
 118 identified by MALDI-TOF-TOF.

119

120

121

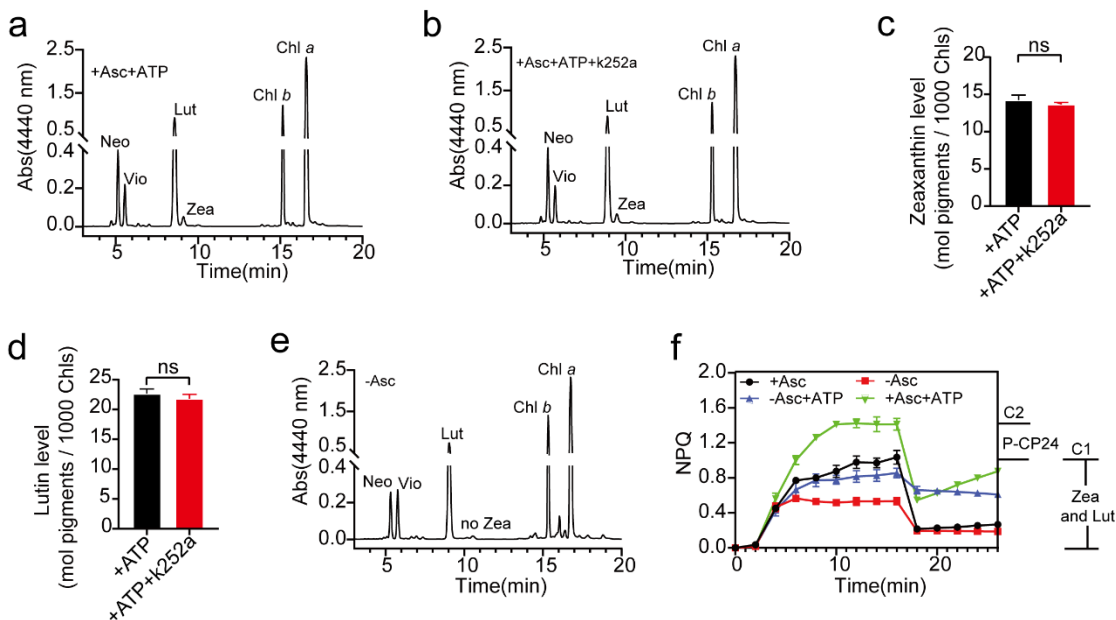
122

123

124

125

126



127

128 **Figure S6: HPLC analysis of total pigments extracted from chloroplasts**

129 **a** Pigments were extracted from functional chloroplasts exposed to HL (1,000  $\mu\text{mol}$  photons  $\text{m}^{-2} \text{s}^{-1}$ ) for  
130 30 min in the absence of k252a, followed by quantification via high-performance liquid chromatography  
131 (HPLC). **b** Pigment were extracted from functional chloroplasts treated with HL (1,000  $\mu\text{mol}$  photons  
132  $\text{m}^{-2} \text{s}^{-1}$ ) for 30 min in the presence of k252a, followed by quantification via HPLC. **c** Zeaxanthin levels  
133 were quantified by HPLC, as shown in **(a)** and **(b)**. **d** Lutein levels were quantified by HPLC, as shown  
134 in **(a)** and **(b)**. The production levels of zeaxanthin and lutein were compared under conditions with or  
135 without the inhibitor k252a using unpaired two-tailed t-tests. Statistical significance was defined as ns ( $p$   
136  $> 0.05$ ), not significant. **e** Pigment were extracted from functional chloroplasts treated with HL of 1,000  
137  $\mu\text{mol}$  photons  $\text{m}^{-2} \text{s}^{-1}$  for 30 min in the absence of Asc, followed by quantification via HPLC. **f** The  
138 contribution decomposition of NPQ induced by actinic light of 1000  $\mu\text{mol}$  photons  $\text{m}^{-2} \text{s}^{-1}$ . NPQ of the  
139 functional chloroplast in the presence of Asc and absence of ATP (+ Asc). NPQ of the functional  
140 chloroplast in the presence of Asc and ATP (+ Asc + ATP). NPQ of the functional chloroplast in the  
141 absence of Asc and ATP (- Asc). NPQ of the functional chloroplast in the presence of ATP and absence  
142 of Asc (- Asc + ATP). The pigment data are normalized to 1000 Chl *a* + *b* molecules. Symbols and error  
143 bars represent the mean  $\pm$  SD calculated from three independent biological replicates.

144

145

146

147

148

149

150

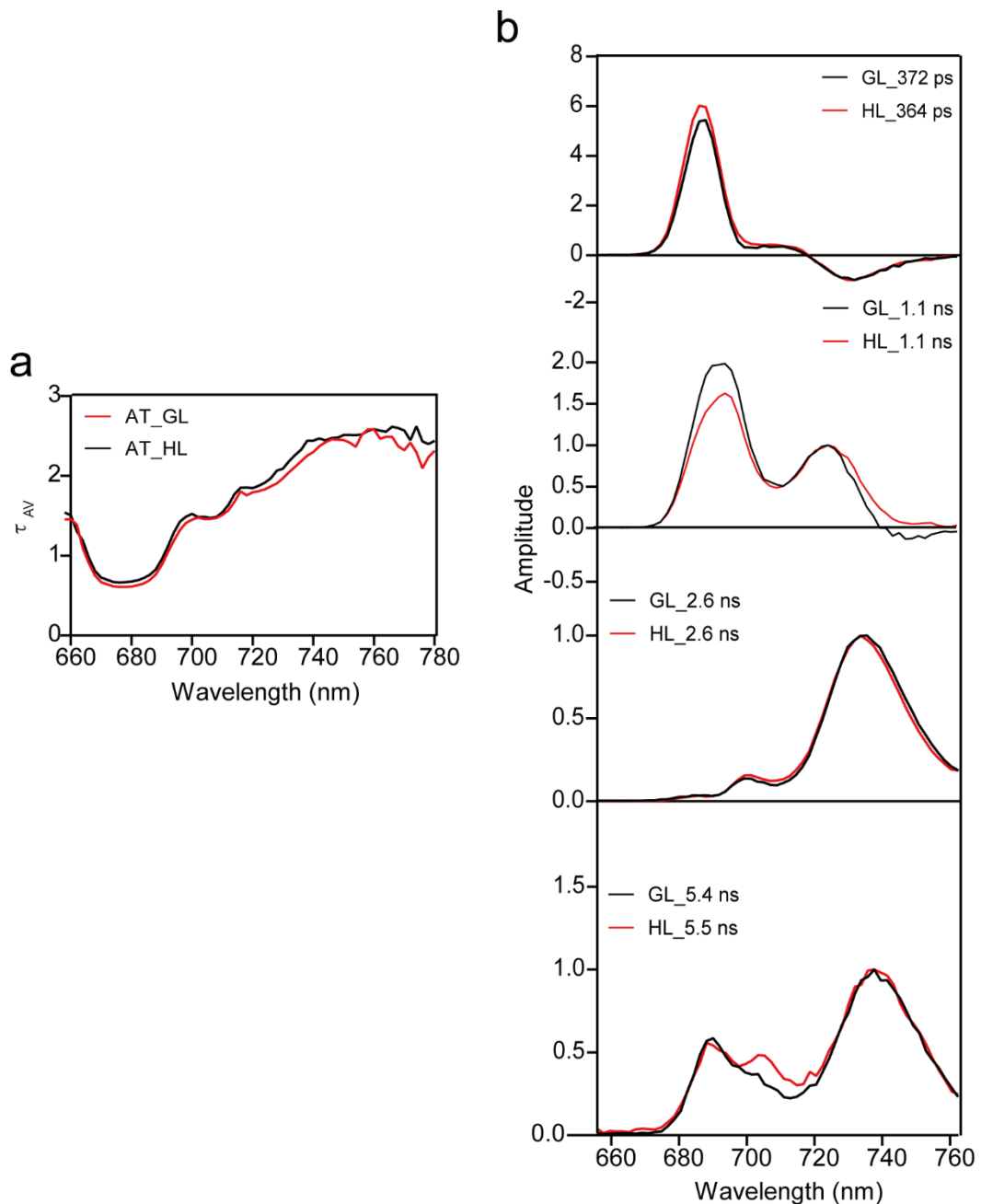
151

152

153

154

155



156

157 **Figure S7: HL does not promote energy dissipation at around 695 nm in *A. thaliana***

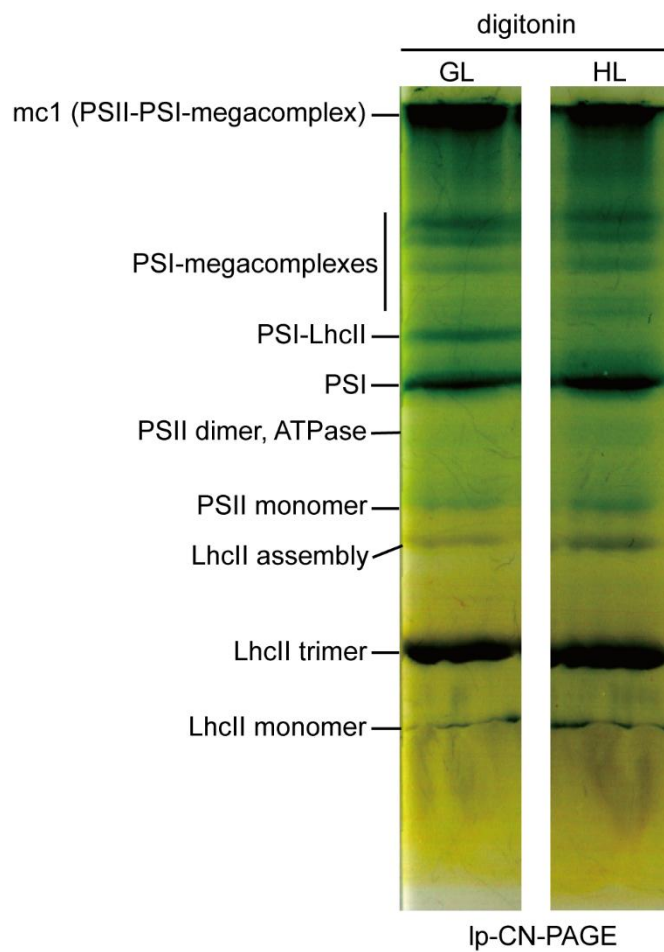
158 **a** Average fluorescence lifetime ( $\tau_{AV}$ ) were measured in thylakoid membranes isolated from *A. thaliana*  
 159 under GL ( $50 \mu\text{mol photons m}^{-2} \text{ s}^{-1}$ ) and HL ( $1000 \mu\text{mol photons m}^{-2} \text{ s}^{-1}$ ) conditions. **b** Time-resolved  
 160 fluorescence decay-associated spectra (DAS) analysis was performed on thylakoid membranes isolated  
 161 from *A. thaliana* grown under GL ( $50 \mu\text{mol photons m}^{-2} \text{ s}^{-1}$ ) and HL ( $1000 \mu\text{mol photons m}^{-2} \text{ s}^{-1}$ )  
 162 conditions. DAS components were normalized to the maximum fluorescence intensity of the  
 163 corresponding PSI-associated lifetime components. Samples were excited at 480 nm with a chlorophyll  
 164 concentration of  $2 \mu\text{g mL}^{-1}$ .

165

166

167

168



169

170 **Figure S8: LpCN-PAGE profiles of thylakoids from *B. incana***

171 Thylakoids were isolated from *B. incana* leaves exposed to either GL (50  $\mu\text{mol}$  photons  $\text{m}^{-2} \text{s}^{-1}$ ) or HL  
 172 (1000  $\mu\text{mol}$  photons  $\text{m}^{-2} \text{s}^{-1}$ ) for 2 hours. Isolated thylakoids were solubilized with 1% (v/v) digitonin  
 173 (final concentration) and subjected to IpCN-PAGE. For each lane, 10  $\mu\text{g}$  of Chl was loaded.

174

175

176

177

178

179

180

181

182

183

184

185

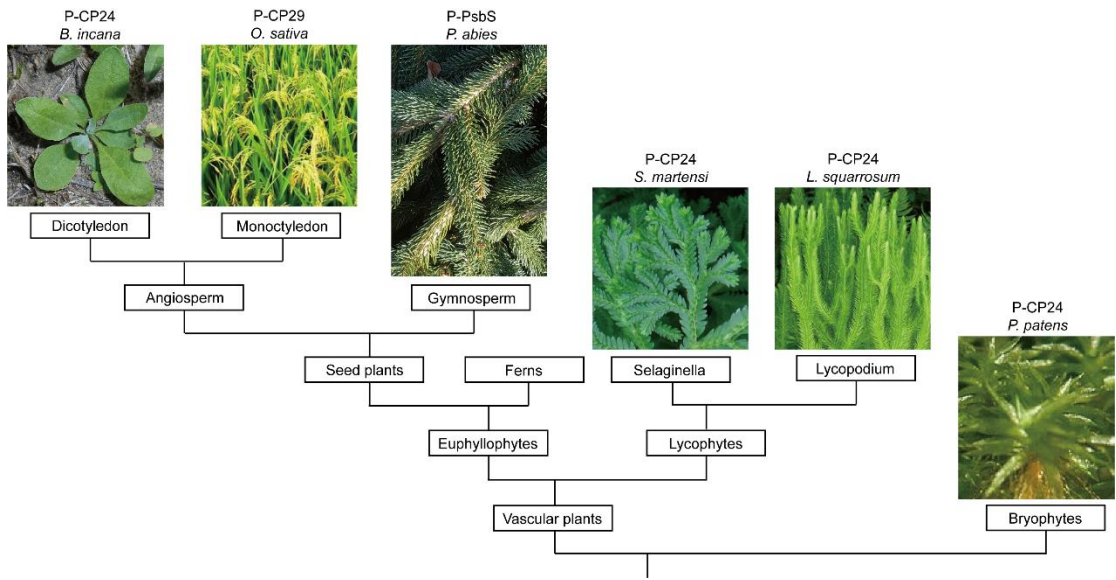
186

187

188

189

190



191

192 **Figure S9: Evolutionary reduction of terrestrial plant phylogeny reveals lineage-specific**  
193 **phosphoprotein signatures.**

194 The latter group comprises non-vascular plants, specifically bryophytes (including mosses and  
195 liverworts), and vascular plants. Among mosses, *P. patens* exhibits extensive phosphorylation of CP24,  
196 though its functional significance remains unclear. Within vascular plants, the earliest phylogenetic  
197 divergence separates lycophytes from euphyllophytes. The lycophyte lineage includes two major clades:  
198 *Selaginella* (spikemosses) and *Lycopodium* (club mosses), which exhibit substantial CP24  
199 phosphorylation. Euphyllophytes consist of ferns and their allies, along with all seed plants. Seed plants  
200 are further classified into angiosperms and gymnosperms. Angiosperms are divided into dicotyledons  
201 and monocotyledons. The dicotyledonous plant *B. incana* studied in this work represents the first seed  
202 plant reported to exhibit substantial CP24 phosphorylation. In contrast, substantial CP29 phosphorylation  
203 has been documented in the monocotyledon *O. sativa*. In gymnosperms, substantial phosphorylation of  
204 PsbS has been detected in the Norwegian spruce (*P. abies*).